Development 130, 1203-1213
© 2003 The Company of Biologists Ltd
doi:10.1242/dev.00319

A mosaic genetic screen for genes necessary for *Drosophila* mushroom body neuronal morphogenesis

John E. Reuter[1,*], Timothy M. Nardine[1,*], Andrea Penton[1], Pierre Billuart[1], Ethan K. Scott[1], Tadao Usui[2], Tadashi Uemura[2,3] and Liqun Luo[1,†]

[1]Department of Biological Sciences, Stanford University, Stanford, CA 94305, USA
[2]Laboratory of Molecular Genetics, Institute for Virus Research, Kyoto University, Sakyo-ku, Kyoto 606-8507, Japan
[3]Core Research for Evolutional Science and Technology (CREST), Japan Science and Technology, Institute for Virus Research, Kyoto University, Kyoto 606-8507, Japan
*These authors contributed equally to this work
†Author for correspondence (e-mail: lluo@stanford.edu)

Accepted 26 November 2002

SUMMARY

Neurons undergo extensive morphogenesis during development. To systematically identify genes important for different aspects of neuronal morphogenesis, we performed a genetic screen using the MARCM system in the mushroom body (MB) neurons of the *Drosophila* brain. Mutations on the right arm of chromosome 2 (which contains ~20% of the *Drosophila* genome) were made homozygous in a small subset of uniquely labeled MB neurons. Independently mutagenized chromosomes (4600) were screened, yielding defects in neuroblast proliferation, cell size, membrane trafficking, and axon and dendrite morphogenesis. We report mutations that affect these different aspects of morphogenesis and phenotypically characterize a subset. We found that *roadblock*, which encodes a dynein light chain, exhibits reduced cell number in neuroblast clones, reduced dendritic complexity and defective axonal transport. These phenotypes are nearly identical to mutations in dynein heavy chain *Dhc64* and in *Lis1*, the *Drosophila* homolog of human lissencephaly 1, reinforcing the role of the dynein complex in cell proliferation, dendritic morphogenesis and axonal transport. Phenotypic analysis of *short stop*/*kakapo*, which encodes a large cytoskeletal linker protein, reveals a novel function in regulating microtubule polarity in neurons. MB neurons mutant for *flamingo*, which encodes a seven transmembrane cadherin, extend processes beyond their wild-type dendritic territories. Overexpression of Flamingo results in axon retraction. Our results suggest that most genes involved in neuronal morphogenesis play multiple roles in different aspects of neural development, rather than performing a dedicated function limited to a specific process.

Key words: Axon, Dendrite, Polarity, Cytoskeleton, Pleiotropy

INTRODUCTION

The establishment of functional neural circuits is dependent on the generation and differentiation of individual neurons. After neurons are born, they undergo a series of morphological changes that include growth, guidance and branching of axons; elaboration of dendritic trees; and synapse formation. Although numerous genes have been implicated in regulating these different steps, systematic identification of new genes essential for neuronal morphogenesis will further our knowledge of the developmental program that helps to assemble neural circuits.

In theory, forward genetic screens can be used to identify genes essential for all aspects of neuronal morphogenesis. However, many genes important for the morphological development of neurons may also be required for similar processes in other cells. Thus, in a multicellular organism that is homozygous mutant for a pleiotropic gene, defects in many cell types and developmental processes are to be expected. It may be difficult to distinguish whether defects in a particular cell type are caused by autonomous or non-autonomous gene disruption. Moreover, development may be arrested in early embryonic stages before neuronal development occurs. Screening genetic mosaics, in which only a small fraction of cells are homozygous mutant for a gene of interest (Xu and Rubin, 1993; Newsome et al., 2000), helps overcome difficulties associated with a traditional screen.

The MARCM (mosaic analysis with a repressible cell marker) system allows positive labeling of mutant cells in mosaic animals thus facilitating genetic analysis of neuronal morphogenesis (Lee and Luo, 1999). We have used the *Drosophila* mushroom body (MB), the insect center for olfactory-mediated learning and memory (Davis and Han, 1996; Heisenberg, 1998), as a model system for such studies. In *Drosophila*, there are three major classes of mushroom body intrinsic neurons called Kenyon cells or MB neurons: γ, α′/β′, and α/β neurons (Crittenden et al., 1998). Each hemisphere contains four MB neuroblasts, with each neuroblast giving rise

to all three major types of neurons (Ito et al., 1997) that are distinguished by morphological characteristics and by birth order during development. MB neurons born in embryos and early larvae belong to the γ class; in late larvae to the α′/β′ class; and after puparium formation to the α/β class (Lee et al., 1999). Each MB neuron sends an initial process that gives rise to dendritic branches in the calyx. The MB axon then fasciculates tightly with other MB axons in the peduncle that extends towards the anterior brain, where each axon then bifurcates, sending one branch towards the midline and another branch dorsally (Fig. 1A) (Lee et al., 1999). During metamorphosis, γ class MB neurons prune their larval-specific axon branches and re-extend only the medial branches that give rise to the adult γ lobe (Fig. 1A). MB neurons have been used as a model system to analyze candidate genes for their function in different aspects of neuronal morphogenesis (for reviews, see Lee and Luo, 2001; Jefferis et al., 2002).

We describe a genetic screen to isolate genes required for neuronal morphogenesis in larval MB neurons. From examining MARCM clones generated on chromosome arm 2R in 4600 independent lines mutagenized with EMS, we identified 33 mutations that cause defects in neuroblast proliferation, cell size, membrane trafficking, and axonal and dendritic morphogenesis. Our study provides new insights into the functions of three previously identified genes and starting points to study axonal and dendritic morphogenesis further using newly identified genes.

MATERIALS AND METHODS

Genetic screen

We began our MARCM-based genetic screen of mutations on chromosome arm 2R (~1000 lines) using a pan-neuronal driver GAL4-C155 to visualize MB clones. Taking advantage of a report that young larvae raised solely on sugar nutrients show preferential cell division in the gonads and MB neuroblasts (Britton and Edgar, 1998), we sought to increase the specificity of generating MB clone by feeding young larvae grape-juice agar. We induced mitotic recombination via heat shock for 1 hour in a water bath at 37°C, adding standard media 24 hours after heat shock. The frequency of non-MB clones was decreased but not eliminated by these efforts.

We then screened another ~3600 chromosomes using the GAL4-201Y driver, which specifically labels MB γ neurons in larvae (Lee et al., 1999). Males carrying isogenized second chromosomes homozygous for *FRTG13, GAL4-201Y, UAS-mCD8-GFP* were treated with 25-40 mM EMS and mated according to the genetic scheme illustrated in Fig. 1B. After a pre-laying period of 3 days, flies were transferred to fresh wet-yeasted vials. Eight hours later, the parents were transferred back to their original vials and kept at 18°C for eventual recovery of mutagenized chromosomes exhibiting MB clonal phenotypes. Twenty-four hours later, newly hatched larvae in the new vials were heat shocked for 60 minutes at 37°C. Brains were dissected from wandering third instar larvae and viewed in a Nikon E-600 compound fluorescence microscope.

We used a third pan-MB GAL4 driver, GAL4-OK107 (Lee et al., 1999), to retest putative mutants. All clones shown in this paper were visualized using the GAL4-OK107 driver.

Deficiency mapping and complementation testing

Although MBs are not required for viability, it is likely that genes involved in MB neuronal morphogenesis are required in other neurons that are essential for viability. We made the assumption that mutations in such genes would be homozygous lethal and thus amenable to complementation mapping. Indeed the vast majority of our mutations were homozygous lethal. This allowed us to map these mutations using the 2R deficiency kit from the Bloomington Stock Center, followed by mapping with small deficiencies, and eventually with candidate genes in the region of the lethal mutation. It is important to note that there could be other background lethal mutations on the mutagenized chromosome that are unrelated to the mutation that causes the observed phenotype.

Non-complementation screen for new alleles of *heron* and *kali*

To identify additional alleles of *heron* and *kali*, we screened mutagenized lines for failure to complement the original mutants. Males homozygous for *cn, bw* were mutagenized (*) as described above and mated en masse to *y, w; Pin/CyO, P[y+]* virgins. F_1 males of the genotype *cn, bw, */CyO, P[y+]* were mated to either *w; FRTG13, UAS-mCD8-GFP, hrn^1/CyO* or *y, w; FRTG13, GAL4-201Y, UAS-mCD8-GFP, kali^1/CyO, P[y+]* virgin females.

Four lines (out of 1133 tested) failed to complement *hrn^1*. These fell into three lethal complementation groups. When recombined with *FRTG13*, only one complementation group containing a single allele recapitulated the phenotype of reduced cell number and overextended dendrites. We named this allele *hrn^2*. Based on its rate of recombination with *FRTG13* (12/66=18.2%), we estimate (with 95% confidence) that *hrn* is located between 48E and 55A. As *hrn^1* was complemented by all available deficiencies in that region, we presume that it is located in one of the regions not covered by the deficiency kit: 48C-48E, 50C-51A, 52F-54B or 54C-54E.

Five lines (out of 1683 lines screened) failed to complement *kali^1*. None showed the dendritic overextension phenotype after clonal analysis. One possibility is that *kali* is not homozygous lethal.

Sample preparation and microscopy

Third instar larvae and adult brains were fixed, washed, antibody stained, mounted, imaged and processed as previously described (Lee and Luo, 1999; Lee et al., 2000b; Ng et al., 2002).

RESULTS AND DISCUSSION

The genetic screen is indicated in Fig. 1B (see also Materials and Methods). The MARCM system permits visualization of homozygous mutant neurons (Lee and Luo, 1999). As MB-GAL4s were used for the majority of these studies, homozygous mutant cells generated outside the MBs would not be labeled. Generation of these non-MB clones was minimized by our selection of a heat shock window at newly hatched larvae, when the only dividing neuroblasts (and thus likely targets of mitotic recombination) are MB neuroblasts and a lateral neuroblast far from the MB neurons (see Ito and Hotta, 1992; Lee and Luo, 1999). In our limited studies using the pan-neuronal GAL4-C155 (the first 1000 lines in the screen), we did encounter other clones occasionally, but they tended to be distant from the MB neurons and their projections. Therefore the consistent phenotypes we observe in labeled MB neurons are most likely caused by disruption of genes acting cell-autonomously in MB neurons.

Three types of clones were expected, based on the neuroblast division pattern in the MB lineage: neuroblast, two-cell and single-cell clones (Fig. 1C). We observed all three types of MB clones in this screen. As previously reported, Nb clones predominated (Lee and Luo, 1999), most probably because perdurance of GAL80 protein in two-cell or single-cell clones weakens GAL4-induced marker expression. The majority of

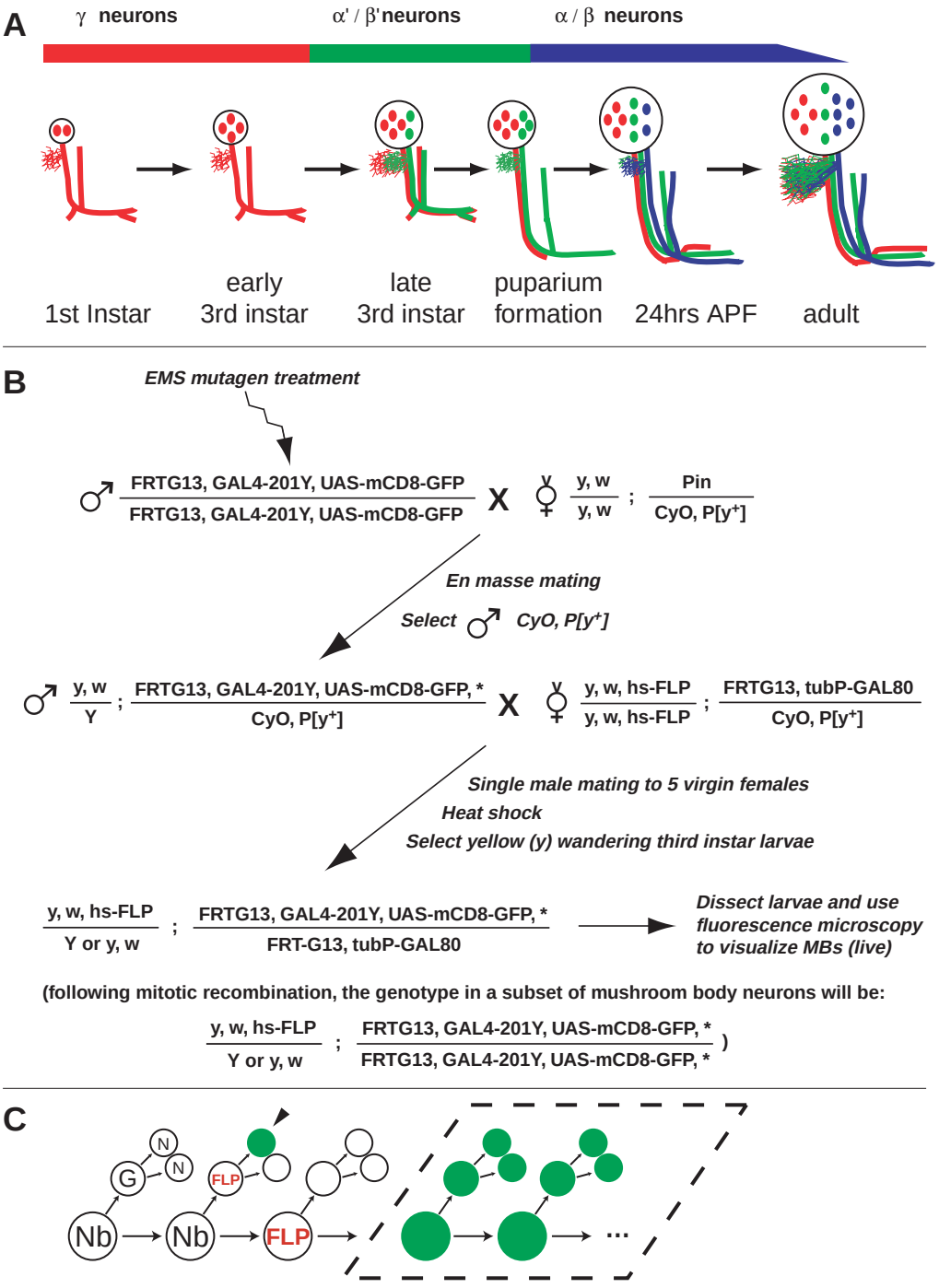

Fig. 1. (A) Schematic of mushroom body development [adapted, with permission, from Lee et al. (Lee et al., 1999)]. The three colors represent three classes of MB neurons born at different developmental windows as indicated. (B) Schematic of the genetic scheme for MARCM-based mosaic screen on chromosome arm 2R. (C) Three types of labeled MARCM clones of MB neurons can be generated by heat-shock induction of FLP recombinase. If mitotic recombination occurs in a dividing neuroblast (Nb), and if the regenerating neuroblast loses the repressor for marker expression, a labeled neuroblast clone is generated (boxed). If the ganglion mother cell (G) loses the repressor, a two-cell clone is generated (not shown). If mitotic recombination occurs in a dividing ganglion mother cell, one postmitotic neuronal progeny (N) loses the repressor resulting in a single-cell clone (arrowhead).

mutations were identified because of their phenotypes in neuroblast clones.

Genes affecting cell number, membrane protein distribution and cell size

The most frequently observed phenotype was a reduction of MB neurons in neuroblast clones. Neuroblast clones generated in newly hatched larvae and examined in wandering third instar larvae typically contain 150-200 neurons (Fig. 2A). Frequently (about 1 in 10 mutagenized lines), we detected neuroblast clones with 50 or fewer cells. This phenotype could be due to homozygous loss of housekeeping genes that are required for cell division, cell survival or basic metabolic functions in neuroblasts. Owing to the sheer number of such mutations and our interest in more specific aspects of neuronal morphogenesis, we did not pursue mutations whose only detectable phenotype was reduced neuroblast clone size.

Three mutants were initially identified because, in addition to a severe reduction in neuroblast clone size, MB neurons displayed little or no axonal and dendritic projections (Table 1; Fig. 2B). Closer examination revealed that these mutants have axonal and dendritic projections that appear normal, but the membrane-targeted mCD8-GFP marker, which normally labels neuronal cell body and axonal/dendritic processes equally well

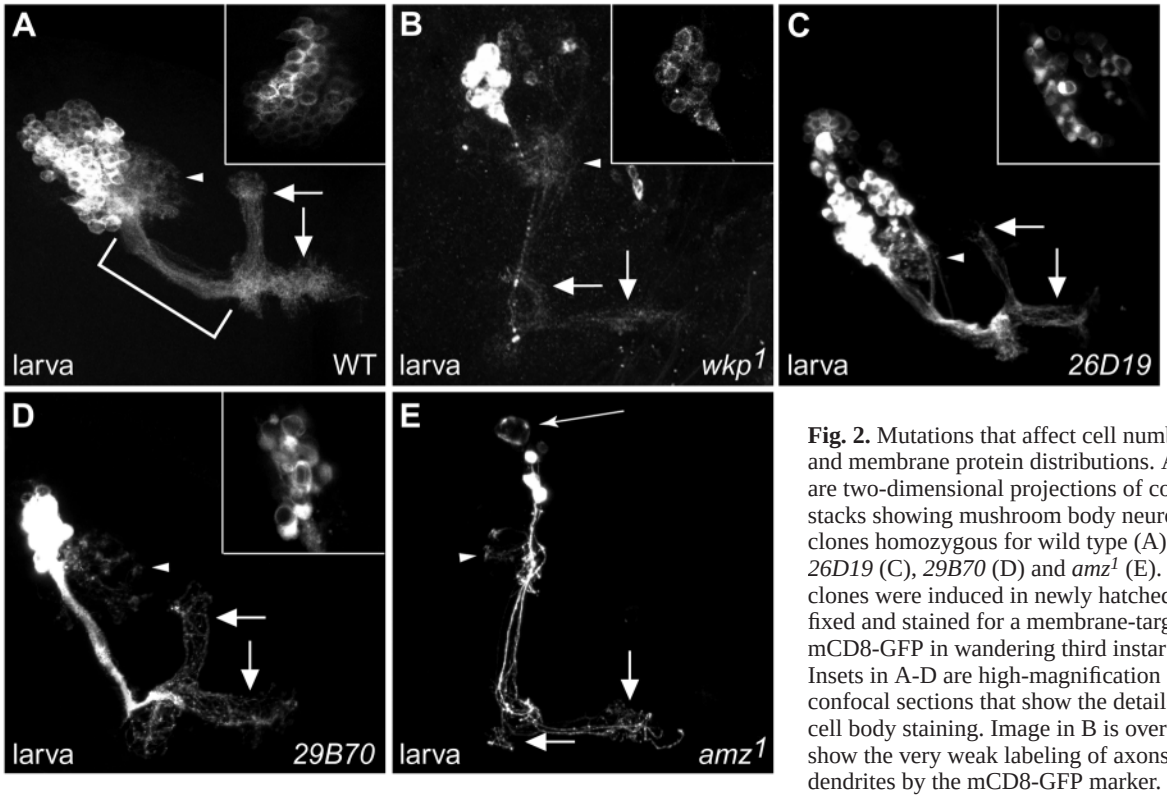

Fig. 2. Mutations that affect cell number, size, and membrane protein distributions. All images are two-dimensional projections of confocal *z*-stacks showing mushroom body neuroblast clones homozygous for wild type (A), *wkp*^{1} (B), *26D19* (C), *29B70* (D) and *amz*^{1} (E). MARCM clones were induced in newly hatched larvae, fixed and stained for a membrane-targeted mCD8-GFP in wandering third instar larvae. Insets in A-D are high-magnification single confocal sections that show the details of the cell body staining. Image in B is overexposed to show the very weak labeling of axons and dendrites by the mCD8-GFP marker. The long arrow in E indicates an abnormally large cell. As the mushroom body is a three-dimensional structure, the dorsal lobe is sometimes almost perpendicular to the X-Y plane because of variation in mounting (see E). In this and all subsequent figures, samples are oriented such that dorsal is upwards and the midline is towards the right. Unless otherwise mentioned, arrowheads point to the calyx, which is the dendritic field of MB neurons. Brackets define the axonal peduncle before branching into the lobes. Horizontal and vertical arrows indicate the dorsal and medial lobes, respectively.

Table 1. A list of mutants identified from this study

Mutants	Number of alleles	Map position
Abnormal membrane marker distribution		
weak processes (*wkp*)	Three	48E-49A
Eight single hits	One each	N.D.
Large cells		
amazon (*amz*)	Two	55A-55C1
11 single hits	One each	N.D.
Spotty axons (defective axonal transport)		
roadblock (robl)	One	54B16
Two single hits	One each	N.D.
Abnormal axon and dendrite morphogenesis		
roadblock (robl)	One	54B16
short stop (shot)	Three	50C6-12
flamingo (fmi)	One	47B6-7
heron (hrn)	Two	See Materials and Methods
kali	One	N.D.

(Lee and Luo, 1999), is now concentrated in cell bodies and was distributed very weakly in axons and dendrites. All three mutations failed to complement deficiencies that span 48E-49A and each other. Based on their nearly identical clonal phenotypes and the lethal complementation data, we conclude that they represent three alleles of the same gene, which we named *weak processes* (*wkp*). Wkp is likely required for efficient transport of membrane protein into axons and dendrites.

We also found a number of mutants (Table 1; Fig. 2C,D) that exhibit abnormal concentration of the mCD8-GFP marker in intracellular structures (Fig. 2C,D, insets), probably reflecting defects in secretory pathways. However, the axonal and dendritic staining was stronger than in clones homozygous for *wkp*.

A third class of mutants exhibit abnormally large cell size in labeled neuroblast clones in addition to a reduction in cell number (Table 1; Fig. 2E). Two of these mutants failed to complement deficiencies within 49C1-50D2 and each other, and are likely to be mutations in the same gene, which we have named *amazon* (*amz*). Complementation tests suggest the remaining mutants may be either single hits or else homozygous viable. Mutations of this class might cause an increase in cell size by affecting cytokinesis, as is the case with *RhoA* mutations (Lee et al., 2000b); however, none of these mutations failed to complement *RhoA*. Alternatively, they could affect genes that regulate cell size (Conlon and Raff, 1999).

roadblock mutations affect axonal transport, neuroblast proliferation and dendritic branching

We identified three mutants that exhibit a ‘spotty axon’ phenotype: neuroblast or single-cell clones homozygous for these mutations have periodic swellings along their axons or near the axon terminals (Fig. 3A). These defects are reminiscent of mutations that affect axonal transport, such as microtubule-based motor protein kinesins (Goldstein and Yang, 2000). We have previously shown that MB neurons

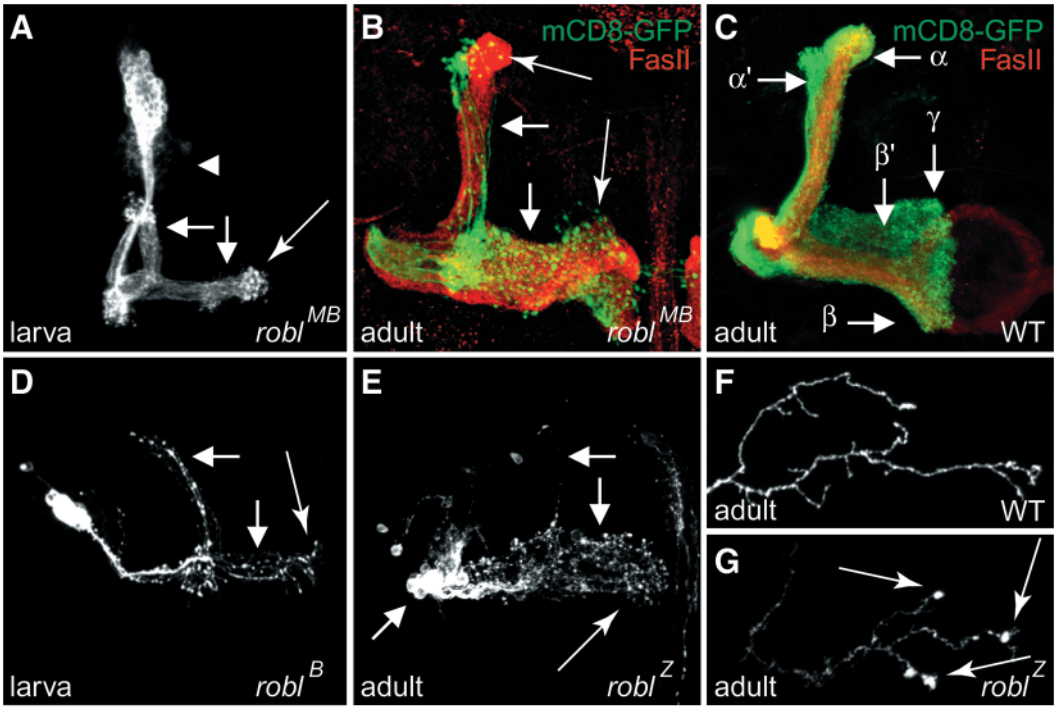

Fig. 3. *roadblock* (*robl*) mutants affect axonal transport and neuroblast proliferation. (A,B) Neuroblast clones homozygous for *robl*^{MB} examined in wandering third instar larva (A) and in adult (B). Red staining in B represents FasII immunoreactivity, which labels strongly the last-born class of α/β neurons. The dorsal axons in *robl*^{MB} neuroblast clones (green) are therefore α′ axons, as they are not stained with FasII. (C) Wild-type mushroom body neuroblast clone double labeled with FasII (red). (D) A *robl*^{B} neuroblast clone examined in wandering third instar larva. (E) A *robl*^{Z} neuroblast clone examined in adult. (F,G) Axons of γ neurons in adult medial lobe from single-cell clones of wild type (F) or *robl*^{Z} (G). Long arrows in all images indicate accumulations of intense mCD8-GFP staining most probably because of accumulation of cargoes along the axons. Short oblique arrow in E indicates the cell body region of this neuroblast clone.

homozygous mutant for genes encoding dynein heavy chain (*Dhc64C*) exhibit similar axon swellings (Liu et al., 2000). Similar phenotypes were also seen in MB neurons homozygous mutant for *Lis1* (Liu et al., 2000), the *Drosophila* homolog of human *LIS1* that has been shown to be associated with the dynein complex (Faulkner et al., 2000; Smith et al., 2000). Haplo-insufficiency of human *LIS1* causes lissencephaly or smooth brain (reviewed by Reiner, 2000). *Dhc64C* and *Lis1* mutations also produce defects in neuroblast proliferation (Liu et al., 2000). Interestingly, one of the new spotty axon mutants, *7A11*, also has similar phenotypes. Additionally, neuroblast clones have reduced cell number compared with wild type (~50 in third instar larva, Fig. 3A). When examined in adults, neuroblast clones homozygous for *7A11* are composed largely of γ neurons, the first-born class of MB neurons (Fig. 1A). They also have few α′/β′ neurons as revealed by double labeling with FasII, which labels α/β neurons strongly and γ neurons weakly, and does not label α′/β′ neurons (Lee et al., 1999) (Fig. 3B). These observations suggest that the reduced size of neuroblast clones is probably caused by a cessation of neuroblast cell division, such that only early born neurons are generated (see Liu et al., 2000).

Deficiency mapping for *7A11* uncovered two lethal mutations at 46E1-F2 and 54C1-4. Of the 29 lethal complementation groups from a previous saturation mutagenesis in the 46C-F region (Goldstein et al., 2001), two alleles in group W failed to complement *7A11*. However, when recombined with *FRTG13*, they did not exhibit a clonal phenotype in MB neurons. Within 54C1-4, we found *roadblock* (*robl*), which encodes a dynein-light chain shown to be required for axonal transport and mitosis (Bowman et al., 1999). Given the phenotypic similarity between *7A11* and *Lis1*/*Dynein heavy chain*, we tested known *robl* mutants (Bowman et al., 1999) and found that two loss-of-function alleles (*robl*^{B} and *robl*^{Z}) failed to complement *7A11*. MARCM clones for both alleles also showed reduced cell number and spotty axons at the larval and adult stages (Fig. 3D,E). Both alleles have stronger phenotypes than *7A11* in that neuroblast clone size is reduced further and the severity of axonal swellings is greater. We therefore concluded that the *7A11* phenotypes we observe are due to a hypomorphic mutation in the *robl* gene, and renamed our mutation *robl*^{MB}.

In addition to affecting neuroblast proliferation and axonal transport, Lis1 and Dynein heavy chain mutants also cause defects in dendritic growth and branching of MB neurons (Liu et al., 2000). To examine whether *robl* also affects dendritic morphogenesis, we quantified dendritic length and branching points in single-cell clones homozygous for *robl*^{Z} in adult. Compared with wild type, we found a twofold reduction in both total dendritic length [*robl*^{z}: 54±11 μm, n=4; wild type: 106±11 μm, n=6; P=0.0061 (t-test)] and branching points [*robl*^{z}: 6.0±0.9, n=4; wild type: 12±1.7, n=6; P=0.0187 (t-test)], demonstrating that, like *Lis1* and *Dhc64C* (Liu et

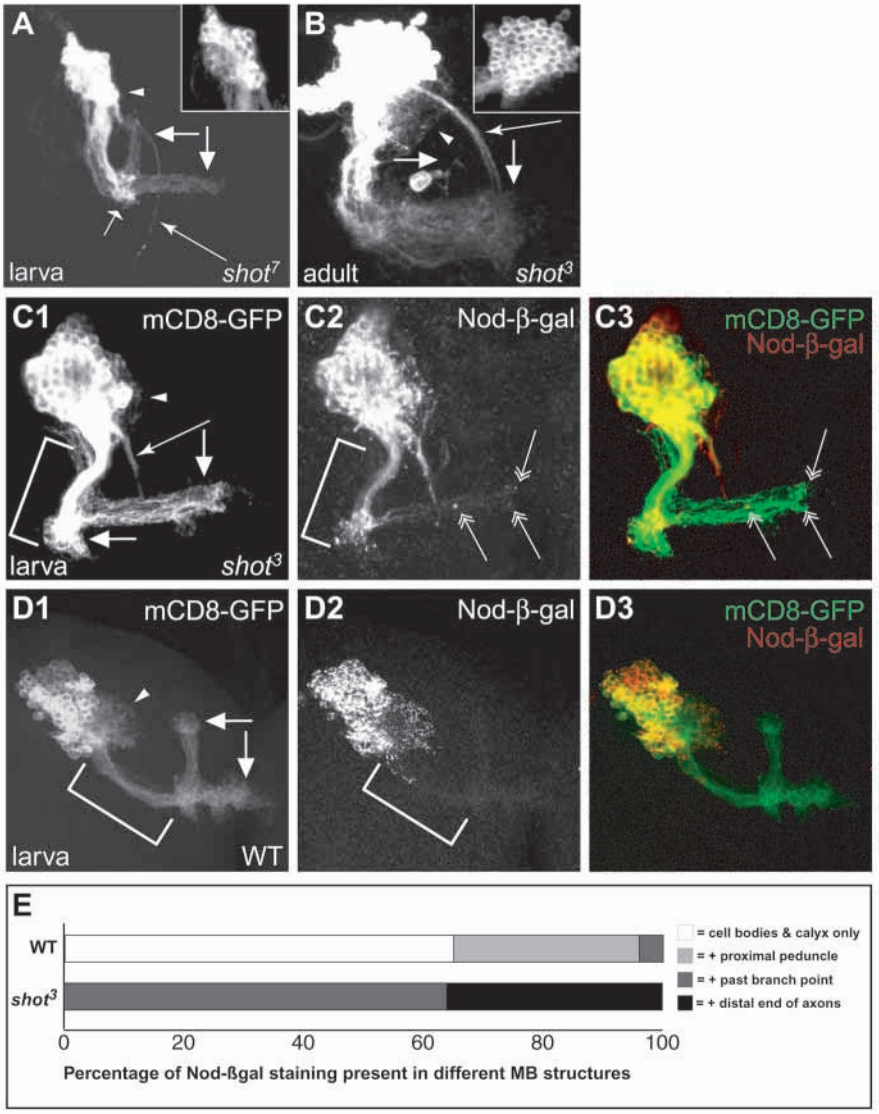

Fig. 4. *short stop* mutants cause multiple defects including neuronal polarity. (A,B) neuroblast clones homozygous for *shot* examined in larva (A) and adult (B). Long arrows point to overextended processes from the calyx. Short oblique arrow in A indicates axon termination in the peduncle as the intensity of mCD8-GFP staining progressively decreases as axons enter the lobe. Both images are overexposed to show the weak axonal lobes (composed of only the early-born γ neurons; the horizontal arrow indicates where the dorsal lobes should be) and the long arrow indicates the overextension from the calyx. Insets show the normal exposure of the cell body region. (C,D) Neuroblast clones with single staining of mCD8-GFP (C1,D1), Nod-βgal (C2,D2) and double labeling (C3,D3) for *shot*^{3} (C) and wild type (D). In wild type, Nod-βgal is confined to the cell bodies, calyx and sometimes the proximal part of the peduncle. In *shot*^{3} neuroblast clones, Nod-βgal often intensely labels the entire peduncle and sometimes can be seen in the axonal lobes and distal end of the axons (double arrows in C, middle and right panels). Overextensions from the dendritic field (long arrow) are also strongly labeled with Nod-βgal. (E) Quantification of the Nod-βgal mislocalization phenotype. *n*=23 for wild type and *n*=14 for *shot*^{3}.

al., 2000), *robl* is cell-autonomously required for dendritic branching and growth.

Although dynein heavy chain and Lis1 exhibit very similar phenotypes, consistent with their forming a complex involved in dynein-mediated function (Reiner, 2000), we have previously found that there was a subtle difference in the axonal transport phenotype. Although the axon swellings are concentrated at the distal ends of axon branches in *Dhc64C* mutant MB neurons, consistent with dynein mediating retrograde axonal transport, swellings in *Lis1* mutant neurons occur along the entire axon (Liu et al., 2000). Axon swellings in single-cell clones of *robl* mutants occur preferentially at the distal ends of axon branches (Fig. 3G, compared with 3F). These observations suggest that the function of *robl* is more central to the function of cytoplasmic dynein, whereas Lis1 may play additional/different functions.

Future phenotypic analysis of two other mutants that exhibit spotty axon phenotypes (Table 1) combined with identification of the corresponding genes may contribute to our understanding of mechanisms of axonal transport, and may elucidate additional components of the Lis1 pathway, which is important for the patterning of the human cerebral cortex.

short stop mutations disrupt neuronal polarity

A number of mutants were identified based on their phenotypes in axonal and dendritic morphogenesis (Table 1). Three mutations share similar phenotypes: MB axon staining becomes progressively weaker further from the cell bodies, suggesting defects in axonal extension. In addition, there are abnormal processes projecting out from the dendritic fields of MB neurons (the MB calyx) (Fig. 4A). These phenotypes are reminiscent of the first characterized mutation with the MARCM method in MB neurons, *short stop* (*shot*) (Lee and Luo, 1999). Indeed all three mutations failed to complement a deficiency that uncovers *shot*; they also failed to complement each other and *shot*^{3}. Based on these genetic criteria and their phenotypic similarity, we conclude that we have identified three new alleles of *shot*, which we named *shot*$^{6\text{-}8}$.

Adult neuroblast *shot*^{3} clones also displayed abnormal

processes projecting out from the calyx (Fig. 4B). They appear to follow a curved route towards the antennal lobe, mimicking the trajectory of the inner antennal cerebral tract (iACT), which contains the axons of a large subset of projection neurons, the major input to the MB dendrites (Stocker et al., 1990; Jefferis et al., 2001).

In addition to these overextension phenotypes, neuroblast clones homozygous for *shot*^{3} (Fig. 4B), as well as for the alleles we identified (data not shown) exhibit significantly reduced cell number. Most or all neurons are γ neurons, as their axons project to the γ lobe, suggesting a defect in the continuous generation of new neurons from the neuroblast.

Originally identified as a mutation in which embryonic motoneurons fail to reach their targets (Van Vactor et al., 1993), *shot* has subsequently been found to affect CNS and PNS axon growth (Kolodziej et al., 1995; Lee et al., 2000a) and dendritic morphogenesis (Gao et al., 1999; Prokop et al., 1998) in *Drosophila* embryos. It also is required for morphogenesis of other embryonic and imaginal epithelial and mesodermal tissues (Gregory and Brown, 1998; Lee and Kolodziej, 2002a; Strumpf and Volk, 1998). *shot* is allelic to *kakapo*, which encodes a large cytoskeletal linker protein similar to vertebrate plakin (Gregory and Brown, 1998; Lee et al., 2000a; Strumpf and Volk, 1998). Recent structure-function analysis suggests that the actin and microtubule-binding domains must be present on the same molecule for Shot to function in axon extension (Lee and Kolodziej, 2002b).

We originally characterized *shot* phenotypes in larval MB neuronal morphogenesis based on defects in axon fasciculation and misguidance, as many 'axons' project out of the calyx, rather than following the peduncles (Lee and Luo, 1999). In light of the finding that *shot* also affects dendritic development in the embryonic PNS and CNS (Gao et al., 1999; Prokop et al., 1998), we re-examined the processes projecting from the calyx. A fusion protein made of a microtubule motor Nod and β-galactosidase (Nod-βgal) is highly enriched in MB dendrites and their tips but largely absent from axons (Lee et al., 2000b) (Fig. 4D). We found that the processes projecting out of the calyx stained strongly for Nod-βgal (Fig. 4C). Strikingly, however, in *shot* neuroblast clones, axons that follow the normal route through the peduncle are also strongly labeled for Nod-βgal (Fig. 4C). Sometimes the Nod-βgal fusion protein is present in both the dorsal and medial lobes all the way to their terminals (Fig. 4C,E), despite the fact that total axon staining become progressively weaker as they are further from the cell bodies (reflecting axon growth defects). This is in contrast to wild type, where Nod-βgal staining rapidly diminishes along the axonal peduncle (Fig. 4D,E) (Lee et al., 2000b). These observations suggest that neuronal polarity, as measured by the microtubule polarity in axons and dendrites, is perturbed in *shot* mutants.

In neurons, dendrites normally collect input and axons send output. As such, there are a number of distinctions between these two neuronal processes structurally, functionally and developmentally (Craig and Banker, 1994). In particular, differences in microtubule polarity have been suggested as a hallmark between axons and dendrites. In a number of vertebrate neurons studied so far, microtubules in axons uniformly orient with their plus end pointing distally. By contrast, microtubules in dendrites have both plus-end-distal and plus-end-proximal orientations, the latter population gradually diminishing further away from the cell body (Baas, 1999; Craig and Banker, 1994). Although direct evidence of similar microtubule polarity in invertebrate neurons is lacking, our studies provide two lines of indirect evidence that microtubule distribution in MB neurons is similar to mammalian neurons. First, Nod, a likely minus-end-directed microtubule motor (Clark et al., 1997), when fused with β-gal is highly enriched in MB dendrites but largely absent in MB axons (Lee et al., 2000b) (Fig. 4D). This observation is consistent with the notion that in MB dendrites microtubules are bi-directional, so a minus-end-directed reporter can enter efficiently into the most distal parts of the dendrites, but cannot be efficiently transported along the axons if microtubules are oriented only plus-end distally. Second, dynein is known to be a minus-end-directed microtubule motor. We observed that, in *Dhc64C* mutants (Liu et al., 2000) and now in *robl* mutants (Fig. 3), axon swellings are preferentially located at the distal tips of MB axons. This is consistent with the notion that in MB axons microtubules are distributed with their plus end pointing distally.

Little is known about the establishment of microtubule polarity differences in axons and dendrites during development. Recent experiments in hippocampal cultured neurons have indicated the importance of polarized microtubule distribution in neuronal polarity development and maintenance. A kinesin superfamily member, CHO1/MKLP1, is distributed in dendrites and has the ability to transport minus-end distal microtubules in the dendrites. Disruption of CHO1/MKLP1 by antisense oligonucleotides resulted in failure of dendritic differentiation in young hippocampal neurons (Sharp et al., 1997), and conversion of dendritic processes into axon-like processes in mature neurons (Yu et al., 2000). *shot* mutants appear to have the opposite phenotype: conveying specific dendritic properties to axonal compartments. It will be very interesting in the future to determine how this microtubule/actin cytoskeletal linker protein regulates neuronal polarity in conjunction with proteins such as CHO1/MKLP1.

fmi mutants overextend processes from the dendritic field

We isolated a mutant, *39B17*, in which many processes extend beyond the typical MB dendritic field, often as far as the axon lobes. We quantified the number of short and long (defined as less or more than one calyx diameter, respectively) overextended processes in *39B17* and for wild type (Table 2). Neuroblast clones homozygous for *39B17* have a marked increase of long over-extended processes. Overextended processes from the calyx are also evident in adult, projecting along similar tracks as the iACT as in the case of *shot* mutant neurons (data not shown; see below). Mutant neuroblast clones also have fewer cells than wild type, which becomes more obvious in adult clones. These clones contain neither α nor α′ dorsal lobes, indicating an arrest of neuroblast proliferation before the generation of α′/β′ neurons (data not shown; see below).

Deficiency mapping uncovered a lethal mutation in the 47A1-47D2 region for *39B17*. We tested our mutation for complementation against a mutant allele of *flamingo* (*fmi*), also known as *starry night*, which encodes a seven transmembrane cadherin (Usui et al., 1999; Chae et al., 1999). Loss-of-function

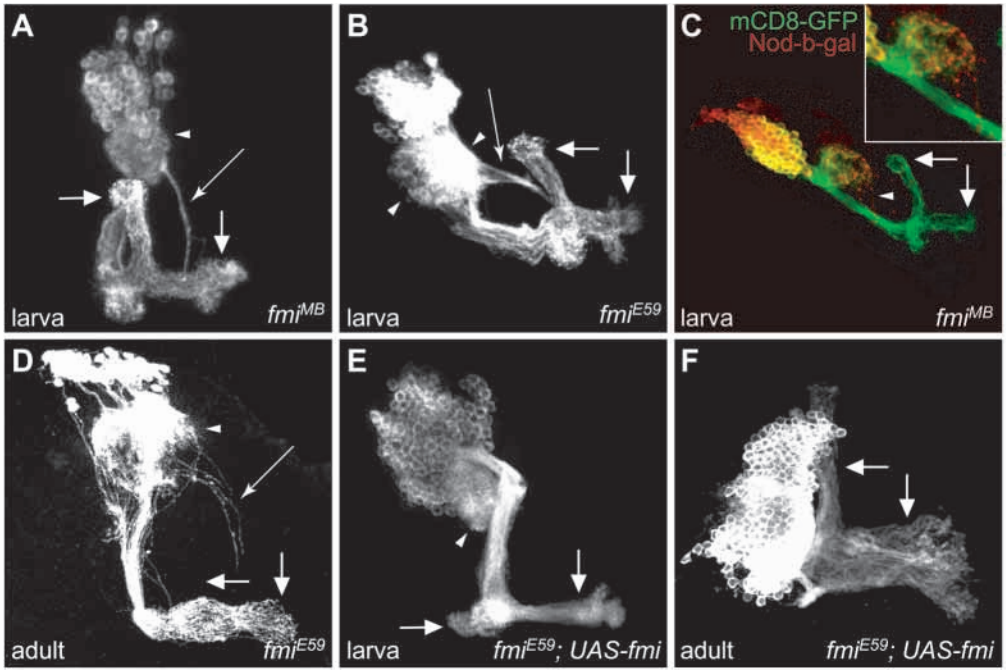

Fig. 5. *flamingo* regulates dendritic extension. (A-C) Larval neuroblast clones homozygous for fmi^{MB} (A) and fmi^{E59} (B) have overextending processes from the calyx (long arrows) that are labeled with Nod-βgal (C, and high magnification in the inset). (D) Adult fmi^{E59} neuroblast clones also have processes that overextend from the calyx (long arrow). In addition, reduction of cell number is evident, as is the lack of the dorsal lobe. (E,F) Clonal expression of *UAS-fmi* (genotype *y,w, hs-FLP, UAS-mCD8-GFP/Y; FRTG13,* fmi^{E59}*/FRTG13, tubP-GAL80; UAS-fmi/+; GAL4-OK107/+*) rescues the phenotypes of dendritic overextension and cell number reduction in both larva (E) and adult (F).

Table 2. Quantification of dendritic overextension in *fmi* and *hrn* mutants

Genotype in neuroblast clones	Total number of clones	Number (percentage) of clones with overextending dendrites	Number (percentage) of clones with long overextending dendrites
Wild type	49	23 (47%)	4 (8.2%)
fmi^{MB}	58	33 (57%)	18 (31%)
fmi^{E59}	39	29 (74%)	23 (59%)
fmi^{MB} + *UAS-fmi*	11	4 (36%)	0 (0%)
fmi^{E59} + *UAS-fmi*	5	1 (20%)	0 (0%)
hrn^{1}	18	14 (78%)	7 (39%)
hrn^{2}	6	4 (66%)	2 (33%)

Long overextension refers to extensions that are greater than the diameter of the calyx.

mutations of *fmi* exhibit defects in planar polarity (Usui et al., 1999; Chae et al., 1999) and excessive dendritic outgrowth and misguidance in embryonic sensory neurons (Gao et al., 1999; Sweeney et al., 2002). *39B17* failed to complement fmi^{E59}, which has a stop codon early in the extracellular domain and is believed to be a null allele (Usui et al., 1999). Two additional lines of evidence demonstrate that the overextension phenotype in *39B17* is due to a mutation in *fmi*. First, MARCM clones of fmi^{E59} also exhibited phenotypes of process overextension and reduction of neuroblast clone size similar to that of *39B17* (Fig. 4D; Table 2). Second, using MARCM, we created MB clones homozygous mutant for fmi^{39B17} or fmi^{E59} in which a full-length *fmi* cDNA was also expressed under the control of UAS; this *UAS-fmi* expression was able to rescue the process overextension and cell number reduction phenotypes in third instar larvae and adults (Fig. 5E,F; Table 2). Thus, our mutation is an allele of *flamingo* and we named this allele fmi^{MB}.

To determine the nature of the overextended processes, we constructed flies carrying $fmi^{MB/E59}$ and *UAS-Nod-βgal*, and made clones using the MARCM system. Nod-βgal staining is observed in a subset of overextended processes (Fig. 5C; data not shown), suggesting that a portion of the overextended processes are dendrites. The remaining overextensions are either misguided axons in the dendritic field or dendrites in which Nod-βgal transport was inefficient.

Fmi has recently been shown to regulate dendritic extension in embryonic and larval sensory neurons (Gao et al., 1999; Gao et al., 2000; Sweeney et al., 2002). *fmi* mutant sensory neurons extend their dorsal dendrites beyond their normal territory. Although dorsal dendrites from homologous neurons appear to repel each other at the dorsal midline in wild type, they do not do so in *fmi* mutants (Gao et al., 2000). Our data extend these previous findings into dendrites of CNS neurons and suggest a general function for *fmi* in regulating dendritic extension.

Fmi overexpression results in axon retraction

While neuroblast clones expressing wild-type Fmi do not exhibit any phenotypes and could indeed rescue the *fmi* mutant phenotypes (Fig. 5E,F), we found that whole MB overexpression of Fmi using GAL4-OK107 results in loss of the dorsal branches of axons when examined in adult (Fig. 6B, compare with Fig. 6A). FasII staining, which allows us to distinguish the three classes of MB neurons (see above), suggests that β, β′ and γ lobes are present when Fmi is expressed in all MB neurons. Coupled

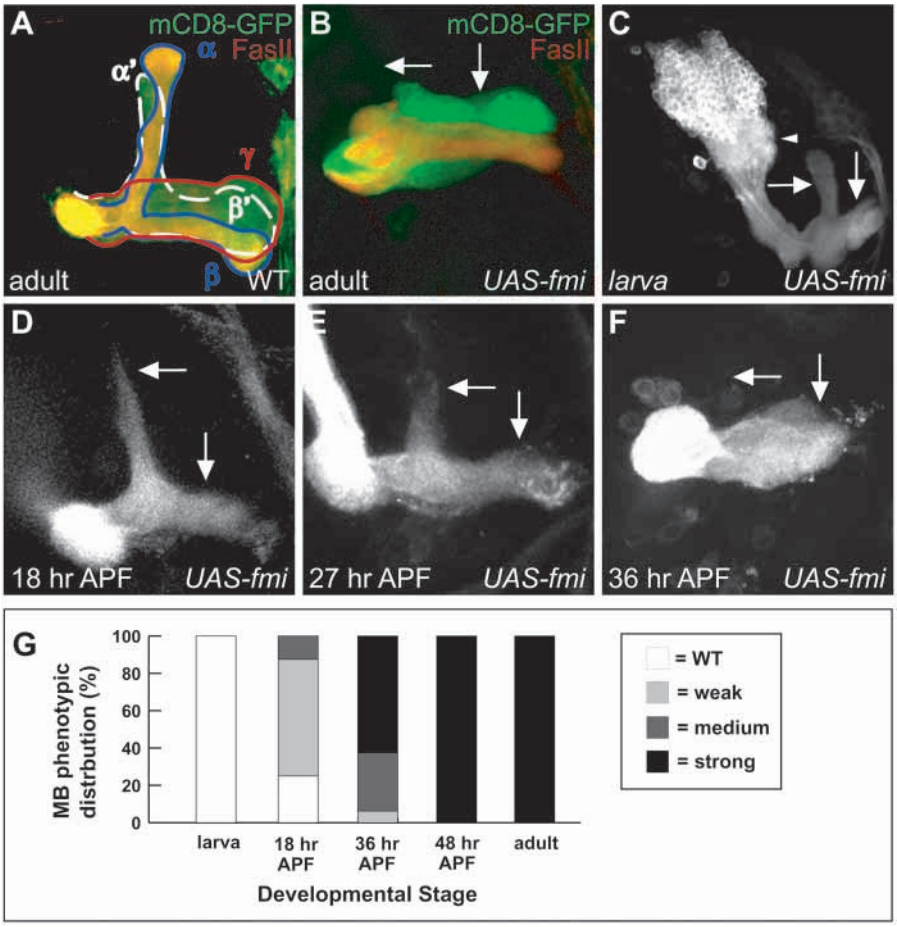

Fig. 6. Flamingo overexpression results in axon retraction. (A) Adult mushroom body axon lobes as visualized by pan-MB expression of mCD8-GFP (green) using GAL4-OK107; double labeled with FasII (in red) (B) Overexpression of Fmi using GAL4-OK107 results in the loss of the dorsal lobe (horizontal arrow). (C-F) Representative images of mushroom bodies overexpressing Fmi at different developmental stages as indicated. APF, after puparium formation. (G) Quantification of dorsal lobe phenotypes. *n*=50, 8, 16, 12, 50 for the five stages quantified. A is adapted from Billuart et al. (Billuart et al., 2001). Copyright (2001), with permission from Elsevier Science.

with the lack of cell loss, we suspect that either the α and α′ axons fail to extend dorsally, or they extend and retract, as is the case for MB neurons expressing double-stranded RNA corresponding to *Drosophila* p190 RhoGAP (Billuart et al., 2001).

To distinguish between these two possibilities, we performed a developmental study and found a progressive worsening of the phenotype. High level expression of Fmi in all MB neurons does not result in any detectable phenotypes in wandering third instar larvae (Fig. 6C). At 18 hours after puparium formation, wild-type MB γ neurons undergo pruning whereas α′/β′ neurons retain their larval branches including the dorsal α′ lobe (Fig. 1A). All MBs overexpressing Fmi retain at least a portion of the dorsal lobes, with 63% more than half the length of the normal dorsal lobe and 25% full length, indicating that at least 25% and perhaps all α′/β′ axons extend normally (Fig. 6D,G). Over the next 12-24 hours, dorsal lobes become progressively shorter until they are not detectable at 48 hours after puparium formation (Fig. 6E-G). Although failure of dorsal lobe extension could in theory also contribute to the phenotypes, these developmental studies indicate that dorsal lobe phenotypes mainly result from axon retraction.

These phenotypes are qualitatively similar to (albeit stronger than) inhibition of p190 RhoGAP (Billuart et al., 2001), which we have previously shown to be caused by activation of RhoA, Drok and phosphorylation of myosin regulatory light change encoded by *spaghetti squash* (*sqh*) (Billuart et al., 2001). We tested whether Fmi may signal through the RhoA/Drok/Sqh pathway. Despite considerable efforts, however, our biochemical studies and genetic interaction experiments failed to provide such a link (A. P., E. K. S. and L. L., unpublished).

The opposite phenotypes (over-extension versus retraction) observed in *fmi* mutant and Fmi overexpression neurons suggest a general role for Fmi as a negative regulator of neuronal process extension.

Two novel genes that affect axonal and dendritic morphogenesis

One mutant, *13B44*, exhibited remarkable phenotypic similarities to *fmi* in many respects. Neuroblast clones homozygous for *13B44* consistently extend their processes out of the calyx and follow the typical arc-like projection (Fig. 7A) found in *fmi* neuroblast clones (Fig. 5A; Table 2). Nod-β-gal staining indicates that this fusion protein is present in the proximal part of some but not all of the overextending processes (Fig. 7B). In addition, we observed a mild reduction of cell number in larval neuroblast clones (Fig. 7A); adult neuroblast clones consist of mainly early born γ neurons, with a few α′/β′ neurons (Fig. 7B).

We recovered a second allele (see Materials and Methods) that exhibited identical clonal phenotypes as the original *13B44* allele (Fig. 7A; Table 2). No deficiency uncovered either allele. We named this new gene *heron* (*hrn*) for its phenotypic similarity with *flamingo* (*stan* – FlyBase).

Another mutant, *41A13*, exhibited a 100% penetrant dendritic overextension phenotype. Unlike *flamingo* or *hrn* mutants, these overextended dendrites project in all directions and are always strongly positive for Nod-βgal (Fig. 7C,D), highly reminiscent of clonal phenotypes for the small GTPase RhoA (Lee et al., 2000b). A complementation screen identified a number of mutations that failed to complement *kali*^{1} but that did not reproduce the *kali*^{1} clonal phenotype.

Future identification of the molecular identity of *hrn* and *kali*, as well as studies of their mechanisms of action including their relationship with Flamingo and RhoA, will further our understanding of the mechanisms that regulate dendritic extension and dendritic field formation.

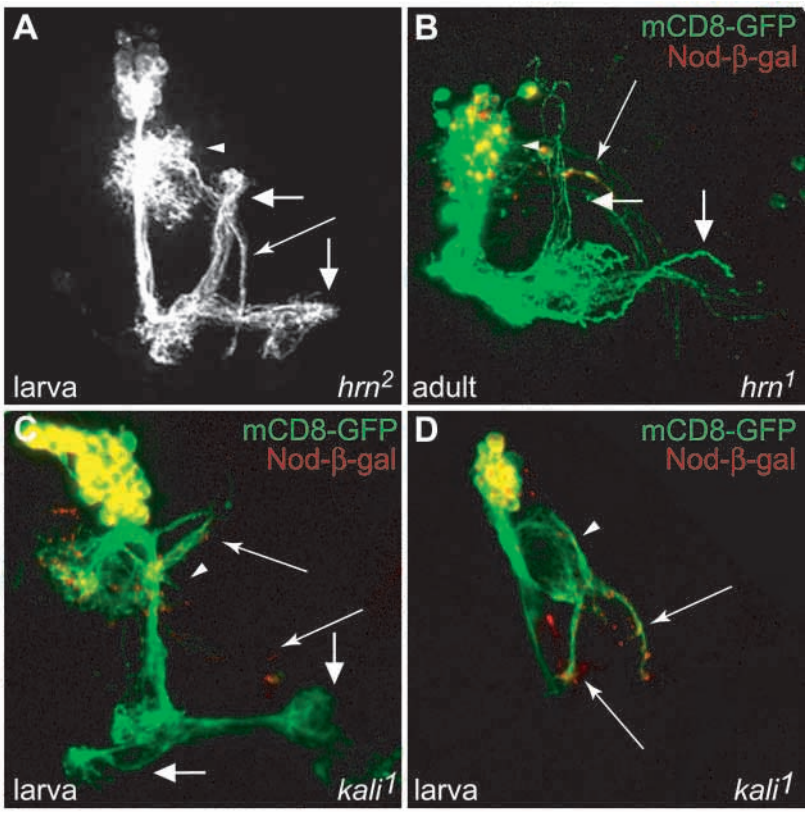

Fig. 7. Phenotypic analysis of *heron* and *kali*. (A) Larval MB neuroblast clones homozygous for *hrn*^{2} results in process extension from the calyx (long arrow). (B) Dendritic overextension persists in *hrn* clones when examined in adult (long arrow). Nod-βgal is distributed in a subset of overextending processes. (C,D) Neuroblast clones homozygous for *kali*^{1} extend processes in all directions from the calyx that are positive for Nod-βgal (long arrows). (D) A partial confocal *z*-stack that removed axonal lobes overlapping the overextended dendrites in the *x-y* plane.

Pleiotropy of gene function in neuronal morphogenesis

In this study, we screened labeled MB clones in 4600 mutagenized lines on chromosome 2R. The majority of mutations we identified are single alleles (Table 1), indicating that the screen is not saturated. However, we did identify multiple alleles for several genes, suggesting that we have sampled a significant proportion of the ~20% of the fly genes located on this chromosome arm.

The ability to visualize mutant cells in a mosaic animal using a method such as MARCM provides great sensitivity in detecting morphological phenotypes. The complex and stereotypical morphogenetic programs of MB neurons further allow us to study different aspects of neuronal morphogenesis. The nature of our mosaic screen allows for identification of pleiotropic genes important for a specific biological process. Interestingly, almost all genes we identified perform multiple functions. All mutations we identified, for example, have reduced cell number in homozygous neuroblast clones examined in adult. Although some could be due to multiple mutations generated on the same chromosome arm, in many cases this is unlikely as the same phenotype is also seen in different alleles in distinct genetic backgrounds, and in one case (*flamingo*) all phenotypes can be rescued by supplying the wild-type transgene. These observations imply that many genes used in the morphological development of MB neurons (and likely other neurons) are used in multiple developmental processes rather than each gene having one specific, dedicated function.

Although mosaic analysis allowed us to identify genes with pleiotropic functions, at the same time the pleiotropy posed a limitation. If the candidate gene is required for and presumably expressed in neural precursors, homozygous mutant clones will inherit the wild-type protein from their heterozygous precursors so they will not lose the gene activity immediately. This perdurance of wild-type protein could prevent identification of genes that function in the early stages of neuronal morphogenesis, such as in the establishment of neuronal polarity or initial axon outgrowth. Perdurance of gene activity could also explain why most of our mutations were isolated based on their defects in neuroblast clones, which presumably dilute the inherited proteins much more rapidly than do single-cell clones.

Hence, it is possible that the nature of our screen precludes identification of proteins that are expressed in neural precursors and are required for early stages of neuronal development. A priori we expected that some genes required for early neuronal differentiation would be turned on only in post-mitotic neurons, negating perdurance issues. Given the scale of our screen and the fact that all the mutations we identified appear to play a role in neuroblast proliferation or survival, it seems likely that most of the genes necessary for differentiation in postmitotic neurons also function in neural precursors. Some of these genes in fact play multiple functions in postmitotic neurons (Table 1). These observations make it essential to couple mosaic analysis such as MARCM with careful phenotypic analysis to unravel the complex process of neuronal morphogenesis.

This work was supported by NIH grants to L. L. and a Human Frontier Science Program grant to L. L. and T. U. We thank members of the Luo laboratory for comments on the manuscript, and thank the Bloomington Stock Center, E. Goldstein and L. Goldstein for mutant stocks.

REFERENCES

Baas, P. W. (1999). Microtubules and neuronal polarity: lessons from mitosis. *Neuron* **22**, 23-31.

Billuart, P., Winter, C. G., Maresh, A., Zhao, X. and Luo, L. (2001). Regulating axon branch stability: the role of p190 RhoGAP in repressing a retraction signaling pathway. *Cell* **107**, 195-207.

Bowman, A. B., Patel-King, R. S., Benashski, S. E., McCaffery, J. M., Goldstein, L. S. B. and King, S. M. (1999). *Drosophila roadblock* and *Chlamydomonas* LC7: a conserved family of dynein-associated proteins involved axonal transport, flagellar motility, and mitosis. *J. Cell Biol.* **146**, 165-179.

Britton, J. S. and Edgar, B. A. (1998). Environmental control of the cell cycle in *Drosophila*: nutrition activates mitotic and endoreplicative cells by distinct mechanisms. *Development* **125**, 2149-2158.

Chae, J., Kim, M. J., Goo, J. H., Collier, S., Gubb, D., Charlton, J., Adler, P. N. and Park, W. J. (1999). The *Drosophila* tissue polarity gene starry night encodes a member of the protocadherin family. *Development* **126**, 5421-5429.

Clark, I. E., Jan, L. Y. and Jan, Y. N. (1997). Reciprocal localization of Nod and kinesin fusion proteins indicates microtubule polarity in the *Drosophila* oocyte, epithelium, neuron and muscle. *Development* **124**, 461-470.

Conlon, I. and Raff, M. (1999). Size control in animal development. *Cell* **22**, 235-244.

Craig, A. M. and Banker, G. (1994). Neuronal polarity. *Annu. Rev. Neurosci.* **17**, 267-310.

Crittenden, J. R., Sloulakis, E. M. C., Han, K.-A., Kalderon, D. and Davis, R. L. (1998). Tripartite mushroom body architecture revealed by antigenic markers. *Learn. Mem.* **5**, 38-51.

Davis, R. L. and Han, K. A. (1996). Neuroanatomy: mushrooming mushroom bodies. *Curr. Biol.* **6**, 146-148.

Faulkner, N. E., Dujardin, D. L., Tai, C. Y., Vaughan, K. T., O'Connell, C. B., Wang, Y. and Vallee, R. B. (2000). A role for the lissencephaly gene LIS1 in mitosis and cytoplasmic dynein function. *Nat. Cell Biol.* **2**, 784-791.

Gao, F. B., Brenman, J. E., Jan, L. Y. and Jan, Y. N. (1999). Genes regulating dendritic outgrowth, branching, and routing in *Drosophila*. *Genes Dev.* **13**, 2549-2561.

Gao, F. B., Kohwi, M., Brenman, J. E., Jan, L. Y. and Jan, Y. N. (2000). Control of dendritic field formation in *Drosophila*: the roles of flamingo and competition between homologous neurons. *Neuron* **28**, 91-101.

Goldstein, E. S., Treadway, S. L., Stephenson, A. E., Gramstad, G. D., Keilty, A., Kirsch, L., Imperial, M., Guest, S., Hudson, S. G., LaBell, A. A. et al. (2001). A genetic analysis of the cytological region 46C-F containing the *Drosophila melanogaster* homolog of the jun proto-oncogene. *Mol. Genet. Genomics* **266**, 695-700.

Goldstein, L. S. B. and Yang, Z. (2000). Microtubule-based transport systems in neurons: the roles of kinesins and dyneins. *Ann. Rev. Neurosci.* **23**, 39-71.

Gregory, S. L. and Brown, N. H. (1998). Kakapo, a gene required for adhesion between and within cell layers in *Drosophila*, encodes a large cytoskeletal linker protein related to plectin and dystrophin. *J. Cell Biol.* **143**, 1271-1282.

Heisenberg, M. (1998). What do the mushroom bodies do for the insect brain? An introduction. *Learn. Mem.* **5**, 1-10.

Ito, K. and Hotta, Y. (1992). Proliferation pattern of postembryonic neuroblasts in the brain of *Drosophila melanogaster*. *Dev. Biol.* **149**, 134-148.

Ito, K., Awano, W., Suzuki, K., Hiromi, Y. and Yamamoto, D. (1997). The *Drosophila* mushroom body is a quadruple structure of clonal units each of which contains a virtually identical set of neurons and glial cells. *Development* **124**, 761-771.

Jefferis, G. S. X. E., Marin, E. C., Stocker, R. F. and Luo, L. (2001). Target neuron prespecification in the olfactory map of *Drosophila*. *Nature* **414**, 204-208.

Jefferis, G. S. X. E., Marin, E. C., Watts, R. and Luo, L. (2002). Development of neuronal connectivity in *Drosophila* antennal lobes and mushroom bodies. *Curr. Opin. Neurobiol.* **12**, 80-86.

Kolodziej, P. A., Jan, L. Y. and Jan, Y. N. (1995). Mutations that affect the length, fasciculation, or ventral orientation of specific sensory axons in the *Drosophila* embryo. *Neuron* **15**, 273-286.

Lee, S. and Kolodziej, P. A. (2002a). The plakin Short Stop and the RhoA GTPase are required for E-cadherin-dependent apical surface remodeling during tracheal tube fusion. *Development* **129**, 1509-1520.

Lee, S. and Kolodziej, P. A. (2002b). Short Stop provides an essential link between F-actin and microtubules during axon extension. *Development* **129**, 1195-1204.

Lee, S., Harris, K. L., Whitington, P. M. and Kolodziej, P. A. (2000a). short stop is allelic to kakapo, and encodes rod-like cytoskeletal-associated proteins required for axon extension. *J. Neurosci.* **20**, 1096-1108.

Lee, T. and Luo, L. (1999). Mosaic analysis with a repressible cell marker for studies of gene function in neuronal morphogenesis. *Neuron* **22**, 451-461.

Lee, T. and Luo, L. (2001). Mosaic analysis with a repressible cell marker (MARCM) for *Drosophila* neural development. *Trends Neurosci.* **24**, 251-254.

Lee, T., Lee, A. and Luo, L. (1999). Development of the *Drosophila* mushroom bodies: sequential generation of three distinct types of neurons from a neuroblast. *Development* **126**, 4065-4076.

Lee, T., Winter, C., Marticke, S. S., Lee, A. and Luo, L. (2000b). Essential roles of *Drosophila* RhoA in the regulation of neuroblast proliferation and dendritic but not axonal morphogenesis. *Neuron* **25**, 307-316.

Liu, Z., Steward, R. and Luo, L. (2000). *Drosophila* Lis1 is required for neuroblast proliferation, dendritic elaboration and axonal transport. *Nat. Cell Biol.* **2**, 776-783.

Newsome, T., Schmidt, S., Dietzl, G., Keleman, K., Asling, B., Debant, A. and Dickson, B. (2000). Trio combines with dock to regulate Pak activity during photoreceptor axon pathfinding in *Drosophila*. *Cell* **101**, 283-294.

Ng, J., Nardine, T., Harms, M., Tzu, J., Goldstein, A., Sun, Y., Dietzl, G., Dickson, B. J. and Luo, L. (2002). Rac GTPases control axon growth, guidance and branching. *Nature* **416**, 442-447.

Prokop, A., Uhler, J., Roote, J. and Bate, M. (1998). The kakapo mutation affects terminal arborization and central dendritic sprouting of *Drosophila* motorneurons. *J. Cell Biol.* **143**, 1283-1294.

Reiner, O. (2000). LIS1. let's interact sometimes... (part 1). *Neuron* **28**, 633-636.

Sharp, D. J., Yu, W., Ferhat, L., Kuriyama, R., Rueger, D. C. and Baas, P. W. (1997). Identification of a microtubule-associated motor protein essential for dendritic differentiation. *J. Cell Biol.* **138**, 833-843.

Smith, D. S., Niethammer, M., Ayala, R., Zhou, Y., Gambello, M. J., Wynshaw-Boris, A. and Tsai, L. H. (2000). Regulation of cytoplasmic dynein behaviour and microtubule organization by mammalian Lis1. *Nat. Cell Biol.* **2**, 767-775.

Stocker, R. F., Lienhard, M. C., Borst, A. and Fischbach, K. F. (1990). Neuronal architecture of the antennal lobe in Drosophila melanogaster. *Cell Tissue Res.* **262**, 9-34.

Strumpf, D. and Volk, T. (1998). Kakapo, a novel cytoskeletal-associated protein is essential for the restricted localization of the neuregulin-like factor, vein, at the muscle-tendon junction site. *J. Cell Biol.* **143**, 1259-1270.

Sweeney, N. T., Li, W. and Gao, F. B. (2002). Genetic manipulation of single neurons in vivo reveals specific roles of flamingo in neuronal morphogenesis. *Dev. Biol.* **247**, 76-88.

Usui, T., Shima, Y., Shimada, Y., Hirano, S., Burgess, R. W., Schwarz, T. L., Takeichi, M. and Uemura, T. (1999). Flamingo, a seven-pass transmembrane cadherin, regulates planar cell polarity under the control of Frizzled. *Cell* **98**, 585-595.

Van Vactor, D., Sink, H., Fambrough, D., Tsoo, R. and Goodman, C. S. (1993). Genes that control neuromuscular specificity in *Drosophila*. *Cell* **73**, 1137-1153.

Xu, T. and Rubin, G. M. (1993). Analysis of genetic mosaics in developing and adult *Drosophila* tissues. *Development* **117**, 1223-1237.

Yu, W., Cook, C., Sauter, C., Kuriyama, R., Kaplan, P. L. and Baas, P. W. (2000). Depletion of a microtubule-associated motor protein induces the loss of dendritic identity. *J. Neurosci.* **20**, 5782-5791.